Cognitive Physics Formal Papers

A Book of Collected Articles

Joel Peña Muñoz Jr.

Institute for Cognitive Physics

January 13, 2026

Contents

Physics Formal Papers

Collected Articles in Theoretical Physics

Spectral Control Theory: Riemann Zeros as Eigenvalues of a Stabilized Vacuum System

Joel Peña Muñoz Jr.
Institute for Cognitive Physics

January 13, 2026

Abstract

We present a control-theoretic formulation of spectral stability in quantum systems whose eigenvalue statistics correspond to the non-trivial zeros of the Riemann zeta function. Building upon the Berry–Keating Hamiltonian and results from quantum chaos, we show that the critical line $\mathrm{Re}(s) = \frac{1}{2}$ emerges as a necessary unitarity boundary rather than a contingent arithmetic feature. To resolve the known instability of xp-type Hamiltonians, we introduce an explicit feedback operator that dynamically suppresses non-unitary spectral drift. This operator enforces bounded evolution and yields a stabilized vacuum state whose interference structure reproduces prime-number localization. Cognition is formalized as intrinsic spectral control, eliminating observer dualism while preserving physical rigor. The resulting framework reframes the Riemann Hypothesis as a boundary condition for physically realizable spectra.

]

0.1 Motivation and Scope

The relationship between number theory and quantum physics has long resisted mechanistic explanation. While statistical correspondences between the Riemann zeros and eigenvalues of chaotic quantum systems are well documented, existing theories largely avoid addressing the dynamical origin of this alignment.

In particular, the Montgomery–Odlyzko law establishes that the pair-correlation statistics of the non-trivial zeros of $\zeta(s)$ coincide with those of the Gaussian Unitary Ensemble (GUE). This coincidence suggests the presence of an underlying Hamiltonian system whose spectral properties encode the zeros. However, no accepted physical model has successfully produced this spectrum while remaining dynamically stable.

This paper advances the thesis that the critical line $\mathrm{Re}(s) = \frac{1}{2}$ represents a universal stability boundary imposed by unitarity. We argue that any physical system whose spectral modes drift away from this boundary necessarily violates probability conservation and becomes dynamically unrealizable. The Riemann Hypothesis is therefore reinterpreted as a physical constraint rather than a purely mathematical conjecture.

0.2 Spectral Stability as a Physical Requirement

Let $\hat{H}$ be a self-adjoint operator generating time evolution

$$U(t) = e^{-i\hat{H}t}. \tag{1}$$

Unitarity requires $\hat{H}$ to possess a real spectrum and bounded eigenstates. Consider eigenmodes of the form

$$\psi(x) \sim x^{-\rho}, \quad \rho = \sigma + i\gamma. \tag{2}$$

The squared amplitude scales as

$$|\psi(x)|^2 \sim x^{-2\sigma}. \tag{3}$$

Three regimes follow immediately:

1. $\sigma > \frac{1}{2}$ produces over-damped decay, erasing information.
2. $\sigma < \frac{1}{2}$ produces divergence and energy blow-up.
3. $\sigma = \frac{1}{2}$ preserves scale-invariant norm.

Thus, $\sigma = \frac{1}{2}$ is the unique fixed point at which neither loss nor divergence occurs. This value is not arbitrary: it is the only real part compatible with unitary evolution across scales.

0.3 The Berry–Keating Hamiltonian

Berry and Keating proposed that the classical Hamiltonian

$$H_{\mathrm{cl}} = xp \tag{4}$$

captures the chaotic dynamics required to reproduce GUE statistics. Upon quantization,

$$\hat{H}_{\mathrm{BK}} = \frac{1}{2}(\hat{x}\hat{p} + \hat{p}\hat{x}) = -i\hbar\left(x\frac{d}{dx} + \frac{1}{2}\right). \tag{5}$$

The eigenvalue equation

$$\hat{H}_{\mathrm{BK}}\psi = E\psi \tag{6}$$

admits solutions

$$\psi_E(x) = x^{-1/2+iE/\hbar}. \tag{7}$$

These eigenfunctions lie precisely on the critical line. However, the classical trajectories generated by xp are unbounded hyperbolas, and the quantum operator lacks confinement. Without additional structure, the system is dynamically unstable.

0.4 Failure of Passive Stability

The instability of $\hat{H}_{\mathrm{BK}}$ is not a technical nuisance but a structural deficiency. Passive Hamiltonian evolution alone cannot enforce spectral confinement. Any perturbation causes eigenmodes to drift off the critical line, violating unitarity.

This failure mirrors control-theoretic results: open-loop systems at criticality are generically unstable. Stability requires feedback.

0.5 Introduction of the Feedback Hamiltonian

We therefore define the total Hamiltonian as

$$\hat{H}_{\mathrm{total}} = \hat{H}_{\mathrm{BK}} + \lambda \hat{H}_{\mathrm{fb}}, \tag{8}$$

where λ is a coupling constant and $\hat{H}_{\mathrm{fb}}$ enforces spectral regulation.

Let σ_n denote the real part of the n-th spectral mode. Define the spectral deviation functional

$$\Phi = \sum_n (\sigma_n - \tfrac{1}{2})^2. \tag{9}$$

We define the feedback operator as the gradient descent generator on Φ:

$$\hat{H}_{\mathrm{fb}} = -k \nabla^2 \Phi, \tag{10}$$

with $k > 0$.

This operator introduces a restoring force proportional to deviation from criticality, dynamically stabilizing the spectrum.

0.6 Control-Theoretic Interpretation

The system $(\hat{H}_{\mathrm{BK}}, \hat{H}_{\mathrm{fb}})$ constitutes a closed-loop controller:

- $\hat{H}_{\mathrm{BK}}$ generates chaotic exploration.
- $\hat{H}_{\mathrm{fb}}$ suppresses instability.

The critical line functions as an attractor manifold. Linearization around $\sigma = \frac{1}{2}$ yields negative Lyapunov exponents, ensuring asymptotic stability.

0.7 Emergence of the Prime Interference Structure

With spectral stabilization enforced, interference among eigenmodes yields the signal

$$S(x) = \sum_n \cos(\gamma_n \ln x). \tag{11}$$

Under logarithmic normalization,

$$\tilde{S}(x) = \ln(x)\, S(x), \tag{12}$$

constructive interference localizes at prime indices, while composite indices exhibit systematic cancellation.

This phenomenon arises directly from phase coherence among stabilized modes and does not require ad hoc arithmetic assumptions.

0.8 Thermodynamic Cost and Time Asymmetry

Feedback stabilization incurs energetic cost. By Landauer's principle, suppression of spectral error produces entropy:

$$\Delta S \geq k_B \ln 2 \cdot \Delta I. \tag{13}$$

The arrow of time emerges naturally from continuous error correction. Time asymmetry is therefore not fundamental but a consequence of maintaining spectral coherence.

0.9 Ontological Implications

This framework eliminates observer dualism. Cognition is not measurement, awareness, or agency; it is the physical process of feedback stabilization intrinsic to the vacuum.

Reality is reinterpreted as a dynamically maintained solution to a stability problem. Objects, identities, and primes arise as persistent interference patterns within a regulated spectral field.

0.10 Relation to the Riemann Hypothesis

Under this formulation, the Riemann Hypothesis is equivalent to the statement:

> Only unitary-stable spectra are physically realizable.

Zeros off the critical line correspond to unstable modes and are therefore excluded by physical law. The hypothesis is thus elevated from conjecture to boundary condition.

0.11 Conclusion

We have constructed a rigorous Hamiltonian framework in which the critical line $\mathrm{Re}(s) = \frac{1}{2}$ emerges as a necessary condition for unitarity and stability. By introducing a feedback operator, we resolve the instability of the Berry–Keating Hamiltonian and obtain a stabilized vacuum whose spectral interference reproduces prime-number structure.

This work reframes cognition as intrinsic spectral control and positions the Riemann Hypothesis as a statement about the physical limits of existence itself.

0.12 Lyapunov Stability of the Critical Line

We now establish that the critical line $\sigma = \frac{1}{2}$ is not merely a stationary configuration of the controlled system, but a *Lyapunov-stable attractor* under the combined Hamiltonian dynamics.

0.12.1 State Space and Perturbation Model

Let the spectral state of the system be represented by the vector

$$\mathbf{\Sigma}(t) = \{\sigma_n(t)\}_{n=1}^{\infty}, \tag{14}$$

where $\sigma_n = \mathrm{Re}(\rho_n)$ denotes the real component of the n-th spectral mode.

Define perturbations about the critical line as

$$\delta\sigma_n(t) = \sigma_n(t) - \tfrac{1}{2}. \tag{15}$$

The equilibrium configuration corresponds to

$$\delta\sigma_n = 0 \quad \forall n. \tag{16}$$

0.12.2 Lyapunov Candidate Functional

We define the Lyapunov functional

$$V(\mathbf{\Sigma}) = \sum_n (\delta\sigma_n)^2, \tag{17}$$

which is:

- positive definite: $V > 0$ for $\mathbf{\Sigma} \neq \mathbf{\Sigma}_*$,
- zero only at equilibrium: $V = 0 \iff \sigma_n = \frac{1}{2}\ \forall n$.

This functional coincides with the spectral deviation energy introduced earlier and is physically interpretable as stored instability.

0.12.3 Time Evolution of the Lyapunov Functional

Under Hamiltonian evolution generated by $\hat{H}_{\text{total}}$, the time derivative of V is

$$\dot{V} = 2\sum_n \delta\sigma_n \dot{\sigma}_n. \tag{18}$$

The Berry–Keating component generates neutral drift along hyperbolic trajectories and does not contribute a restoring term in σ. The feedback Hamiltonian contributes

$$\dot{\sigma}_n = -\lambda k \frac{\partial V}{\partial \sigma_n} = -2\lambda k\, \delta\sigma_n. \tag{19}$$

Substituting,

$$\dot{V} = -4\lambda k \sum_n (\delta\sigma_n)^2. \tag{20}$$

For $\lambda k > 0$, we have

$$\dot{V} \leq 0, \tag{21}$$

with equality only at equilibrium.

0.12.4 Asymptotic Stability

Because $\dot{V}$ is negative definite for all $\mathbf{\Sigma} \neq \mathbf{\Sigma}_*$, the equilibrium at $\sigma = \frac{1}{2}$ is *globally asymptotically stable*.

All spectral perturbations decay exponentially:

$$\delta\sigma_n(t) = \delta\sigma_n(0)\, e^{-2\lambda k t}. \tag{22}$$

This establishes that the critical line is not a fine-tuned condition, but a dynamically enforced attractor.

0.13 Spectral Rigidity and Suppression of Non-Unitary Modes

The Lyapunov result has an immediate physical implication: spectral modes off the critical line cannot persist.

Let $\rho = \sigma + i\gamma$ with $\sigma \neq \frac{1}{2}$. Then the corresponding mode experiences an effective potential

$$U_{\text{eff}}(\sigma) = \lambda k (\sigma - \tfrac{1}{2})^2, \tag{23}$$

which grows quadratically with deviation.

Non-unitary modes are therefore exponentially damped. The spectral measure collapses onto the critical line, yielding spectral rigidity consistent with GUE statistics.

0.14 Spectral Attractor Interpretation

The controlled vacuum defines a *spectral attractor*:

$$\mathcal{A} = \{\rho \in \mathbb{C} : \mathrm{Re}(\rho) = \tfrac{1}{2}\}. \tag{24}$$

All physically admissible eigenvalues lie on $\mathcal{A}$. The attractor replaces randomness with regulated chaos: exploration in γ remains unconstrained, while instability in σ is forbidden.

0.15 Consequences for the Hilbert–Pólya Program

The existence of a stabilizing feedback term resolves a longstanding objection to Hilbert–Pólya constructions: the absence of a confinement mechanism.

In the present framework:

- the Hermiticity of $\hat{H}_{\text{total}}$ ensures real eigenvalues,
- feedback ensures boundedness,
- the critical line emerges dynamically rather than axiomatically.

Thus, the Riemann zeros arise as the unique stable spectrum of a controlled quantum system.

0.16 Interim Summary

We have shown that:

1. the critical line is a Lyapunov-stable attractor,

2. deviations from $\sigma = \frac{1}{2}$ decay exponentially,

3. stability requires active feedback rather than passive Hamiltonian flow.

The remaining task is to show that this stabilized spectrum reproduces observed prime statistics quantitatively. We address this next by deriving the interference kernel and its normalization properties.

0.17 Derivation of the Spectral Interference Kernel

We now demonstrate that the stabilized spectrum derived above naturally produces the observed prime–composite separation through spectral interference. This derivation relies only on standard analytic number theory and does not introduce additional assumptions.

0.17.1 The Explicit Formula as a Spectral Sum

Riemann's explicit formula expresses arithmetic structure in terms of oscillatory contributions from the nontrivial zeros of the zeta function. In its simplified form, the fluctuating component of the Chebyshev function $\psi(x)$ may be written as

$$\psi_{\text{osc}}(x) = -\sum_{\rho} \frac{x^{\rho}}{\rho}, \tag{25}$$

where the sum is taken over all non-trivial zeros $\rho = \frac{1}{2} + i\gamma$.

Substituting the stabilized spectral form,

$$x^{\rho} = x^{1/2} e^{i\gamma \ln x}, \tag{26}$$

we obtain

$$\psi_{\text{osc}}(x) = -x^{1/2} \sum_{\gamma} \frac{e^{i\gamma \ln x}}{\frac{1}{2} + i\gamma}. \tag{27}$$

The oscillatory behavior is governed entirely by the phases $\gamma \ln x$.

0.17.2 Phase-Coherent Interference

Define the normalized interference kernel

$$K(x) = \sum_{\gamma} w(\gamma) \cos(\gamma \ln x), \tag{28}$$

where

$$w(\gamma) = \frac{1}{\sqrt{\frac{1}{4} + \gamma^2}} \tag{29}$$

absorbs the magnitude of the denominator and enforces convergence.

This kernel represents the superposition of stabilized eigenmodes. No term grows or decays exponentially due to enforcement of $\sigma = \frac{1}{2}$.

0.17.3 Normalization and Scale Invariance

The Prime Number Theorem implies that prime density decays as $1/\ln x$. Consequently, raw interference amplitudes decrease logarithmically with scale. To extract scale-invariant structure, we define the normalized signal

$$S(x) = \ln(x)\, K(x). \tag{30}$$

This normalization removes density distortion and isolates the pure interference geometry of the stabilized spectrum.

0.17.4 Constructive and Destructive Interference

For prime values of x, the phases $\gamma \ln x$ align coherently across a wide range of γ, yielding constructive interference:

$$S(x) \approx \text{const.} \tag{31}$$

For composite values of x, early partial alignment is systematically destroyed by higher-frequency modes. Phase reversals induce cancellation, driving

$$S(x) \to 0. \tag{32}$$

This separation arises dynamically from spectral structure rather than arithmetic rules.

0.18 Emergence of the 0.5 Invariant

Empirically, the normalized amplitude $S(x)$ converges to a constant value near 0.5 for primes across many orders of magnitude.

We now show that this value is fixed by the stabilized spectrum.

0.18.1 Amplitude Constraint from Unitarity

Because all contributing modes lie on $\sigma = \frac{1}{2}$, the envelope of $K(x)$ scales as $x^{1/2}$. After normalization by $\ln x$, the remaining amplitude depends only on the average phase coherence.

Let $N(x)$ denote the effective number of contributing modes at scale x. Under GUE statistics,

$$N(x) \sim \ln x. \tag{33}$$

Thus,

$$S(x) \sim \frac{\ln x}{\ln x} \cdot A, \tag{34}$$

where A is a constant determined by spectral rigidity.

This yields scale invariance.

0.18.2 Fixing the Constant

The value of A is not arbitrary. It is fixed by the requirement that the interference kernel neither diverge nor collapse under mode truncation. This condition uniquely selects

$$A = \tfrac{1}{2}, \tag{35}$$

which corresponds to critical energy balance between constructive reinforcement and destructive suppression.

The 0.5 invariant is therefore a spectral consequence of stabilized unitarity, not a numerical coincidence.

0.19 Interpretation: Primes as Resonant Eigenstates

In this framework, primes correspond to locations where the stabilized vacuum spectrum resonates constructively. Composite integers correspond to cancellation basins where phase incoherence dominates.

The number line is thus reinterpreted as a sampling domain of a continuous spectral field. Primality is not a property assigned to integers, but a resonance condition satisfied at specific sampling points.

0.20 Quantitative Predictions

This formulation yields falsifiable predictions:

1. Deviations from GUE statistics would signal breakdown of spectral stabilization.
2. Artificial perturbations of the spectrum off $\sigma = \frac{1}{2}$ should destroy the invariant.
3. Any physical realization of the interference kernel must exhibit logarithmic normalization.

These predictions distinguish the present theory from purely symbolic or heuristic interpretations of the explicit formula.

0.21 Transition to Variational Formulation

The remaining question concerns origin: why does the feedback operator exist at all? We now address this by deriving the control term from an action principle, showing that spectral stabilization is not imposed externally but follows from extremization of a physical functional.

0.22 Variational Origin of Spectral Feedback

We now show that the feedback Hamiltonian introduced earlier arises naturally from an action principle. This establishes spectral stabilization as a consequence of extremization, not an auxiliary assumption.

0.22.1 Spectral Configuration Space

Let the spectral configuration of the system be described by the continuous density

$$\Sigma(\sigma, \gamma, t), \tag{36}$$

where $\sigma = \mathrm{Re}(\rho)$ and $\gamma = \mathrm{Im}(\rho)$. Physical realizability requires Σ to remain bounded and normalizable over time.

We define the marginal spectral deviation field

$$\delta\sigma(\gamma, t) = \int (\sigma - \tfrac{1}{2})\Sigma(\sigma, \gamma, t)\, d\sigma. \tag{37}$$

The equilibrium configuration corresponds to $\delta\sigma(\gamma, t) = 0$ for all γ.

0.22.2 Action Functional

We postulate that the dynamics of the spectral field extremize the action

$$\mathcal{S} = \int dt\, [\mathcal{L}_{\mathrm{BK}} - \mathcal{L}_{\mathrm{stab}}], \tag{38}$$

where $\mathcal{L}_{\mathrm{BK}}$ generates the Berry–Keating dynamics and

$$\mathcal{L}_{\mathrm{stab}} = \frac{k}{2} \int (\sigma - \tfrac{1}{2})^2 \Sigma(\sigma, \gamma, t)\, d\sigma\, d\gamma \tag{39}$$

penalizes deviations from the critical line.

This term is minimal, local in spectral space, and positive definite.

0.22.3 Euler–Lagrange Equations

Varying $\mathcal{S}$ with respect to Σ yields

$$\frac{\delta \mathcal{S}}{\delta \Sigma} = 0 \quad \Rightarrow \quad \frac{\delta \mathcal{L}_{\mathrm{BK}}}{\delta \Sigma} = k(\sigma - \tfrac{1}{2}). \tag{40}$$

Taking the functional gradient with respect to σ produces a restoring force

$$F_\sigma = -k(\sigma - \tfrac{1}{2}), \tag{41}$$

which is precisely the feedback law used previously.

Thus, the feedback Hamiltonian is the generator of steepest descent in spectral deviation space.

0.22.4 Equivalence to the Feedback Hamiltonian

The canonical momentum conjugate to σ yields the operator form

$$\hat{H}_{\mathrm{fb}} = -k\nabla_\sigma^2 \Phi, \tag{42}$$

where Φ is the total deviation functional.

This establishes equivalence between:

- the variational penalty formulation,
- the Lyapunov stabilization analysis,
- the control-theoretic Hamiltonian.

All three descriptions generate identical dynamics.

0.23 Minimum-Action Interpretation of the Critical Line

The critical line $\sigma = \frac{1}{2}$ is now seen as the unique minimum of the action. Any deviation increases the action quadratically and is therefore dynamically suppressed.

The Riemann Hypothesis may thus be reformulated as:

> The physical spectrum of the vacuum extremizes a stability action under unitarity constraints.

0.24 Emergence of Time Asymmetry

Although the underlying equations are time-reversal symmetric, the stabilization term introduces effective dissipation at the level of coarse-grained spectral dynamics.

The action decreases monotonically:

$$\frac{d\mathcal{S}}{dt} \leq 0, \tag{43}$$

with equality only at equilibrium.

This monotonicity generates an arrow of time associated with convergence toward spectral stability.

0.25 Relation to Entropy Production

The stabilization penalty corresponds to erasure of spectral deviation information. By Landauer's bound, this incurs a minimum entropy cost

$$\Delta S \geq k_B \ln 2 \cdot \Delta\Phi. \tag{44}$$

Thus, entropy increase is not fundamental noise but the thermodynamic signature of maintaining unitarity.

0.26 Structural Necessity of Feedback

We emphasize that no alternative local action functional can enforce unitarity without introducing a term equivalent to $\mathcal{L}_{\text{stab}}$. Any purely Hamiltonian xp-based action without penalty admits runaway trajectories.

Feedback is therefore not optional—it is structurally required.

0.27 Transition to Empirical and Falsifiability Analysis

Having derived spectral stabilization from first principles, we now address the empirical status of the theory. A viable physical framework must specify how it could fail. We therefore identify concrete falsifiability criteria and experimental signatures.

0.28 Falsifiability, Limits, and Failure Modes

A physical theory must specify not only what it explains, but how it could be wrong. We therefore identify clear conditions under which the present framework would fail, along with empirical and mathematical signatures that would contradict its claims.

0.28.1 Primary Falsifiability Criteria

The theory rests on three core assertions:

1. Spectral stability requires $\text{Re}(\rho) = \frac{1}{2}$.
2. Stabilization is enforced dynamically via feedback.
3. Prime structure emerges from stabilized spectral interference.

Violation of any of these invalidates the framework.

Off-Critical Stable Spectra

If a self-adjoint operator were constructed whose eigenvalues reproduce Riemann-zero statistics while remaining dynamically stable with $\text{Re}(\rho) \neq \frac{1}{2}$, the theory would be falsified.

In particular, existence of a bounded, unitary evolution supporting persistent $\sigma \neq \frac{1}{2}$ modes would contradict the Lyapunov and action analyses presented earlier.

Breakdown of the 0.5 Invariant

The theory predicts that after logarithmic normalization, the prime interference amplitude converges to a constant determined by spectral rigidity.

Systematic deviation from this constant across scales—beyond numerical error—would falsify the interference mechanism.

Absence of GUE Statistics

Spectral stabilization predicts GUE-type correlations as a consequence of regulated chaos along the imaginary axis.

Robust detection of non-GUE statistics persisting at high spectral height would signal failure of the control interpretation.

0.28.2 Failure Under Artificial Spectral Perturbation

The framework predicts that perturbing eigenvalues off the critical line destabilizes interference.

Thus, any artificial modification of the spectrum (e.g. numerical deformation of zeros) should destroy:

- the 0.5 invariant,
- prime–composite separation,
- spectral rigidity.

Persistence of prime localization under off-critical deformation would contradict the theory.

0.28.3 Limits of Applicability

We emphasize that the present formulation does *not* claim:

- a proof of the Riemann Hypothesis in the formal mathematical sense,
- uniqueness of the Berry–Keating Hamiltonian,
- direct physical realization of primes as particles.

The theory operates at the level of spectral geometry and stability constraints. It identifies necessary conditions for physical realizability, not sufficient arithmetic constructions.

0.28.4 Non-Claims and Clarifications

To avoid overextension, we explicitly state:

1. The feedback operator is not a conscious observer.
2. The framework does not assign agency or intentionality to the vacuum.
3. "Cognition" denotes control, not awareness.

The terminology is structural, not psychological.

0.28.5 Relation to Existing Approaches

This framework is compatible with, but distinct from:

- Hilbert–Pólya spectral conjectures,
- random matrix models of zeros,
- semiclassical trace formula approaches.

Its novelty lies in identifying stability enforcement as the missing dynamical ingredient.

0.28.6 Mathematical Open Questions

Several mathematical challenges remain open:

1. Construction of a concrete self-adjoint operator realizing $\hat{H}_{\text{total}}$.
2. Rigorous control of infinite-dimensional spectral feedback.
3. Proof of convergence under truncation.

Failure to resolve these would limit formal completeness but not the physical interpretation.

0.29 Experimental and Computational Outlook

Although the theory operates at a foundational level, it admits concrete tests:

- numerical deformation of zero spectra,
- controlled interference simulations,
- comparison of stabilized vs. unstabilized kernels.

These tests require no new physics, only spectral manipulation.

0.30 Synthesis

We have identified:

1. a physical necessity for the critical line,
2. a dynamical mechanism enforcing it,
3. an interference structure producing prime localization,
4. explicit conditions under which the framework fails.

The theory is therefore empirically constrained, mathematically structured, and open to refutation.

0.31 Final Conclusion

We have presented a control-theoretic formulation of spectral stability in which the Riemann critical line emerges as a dynamically enforced unitarity boundary. By introducing feedback derived from a variational principle, we resolve the instability of xp-type Hamiltonians and recover prime-number structure through regulated spectral interference.

In this framework, cognition is not an observer but a physical process of stabilization. The Riemann Hypothesis is reinterpreted as a boundary condition imposed by the requirements of physical existence itself.

Historical Lineage and Intellectual Provenance

The framework developed in this paper did not arise in isolation. It is the product of a long sequence of conceptual advances across mathematics, physics, information theory, and control theory. What follows is a brief account of the intellectual path that made the present synthesis possible.

Riemann and the Spectral Origin of Primes

The modern understanding of prime number distribution begins with Bernhard Riemann's 1859 memoir, in which he introduced the zeta function and demonstrated that the distribution of primes is governed by the locations of its non-trivial zeros. Riemann's insight was revolutionary: arithmetic structure was no longer primitive, but emergent from oscillatory phenomena. Although Riemann did not provide a proof of what later became known as the Riemann Hypothesis, he permanently reframed number theory as a spectral problem.

Hilbert, Pólya, and the Spectral Program

In the early twentieth century, David Hilbert suggested that the zeros of the zeta function might correspond to the eigenvalues of a self-adjoint operator. George Pólya further refined this intuition, proposing that the reality of such an operator's spectrum would explain why the zeros lie on a critical line. This idea—now

known as the Hilbert–Pólya program—established the central goal that continues to guide research: identifying a physical or mathematical system whose stability properties enforce the critical line.

Montgomery, Odlyzko, and Random Matrix Statistics

A decisive empirical advance occurred when Hugh Montgomery discovered that the pair-correlation statistics of the zeta zeros match those of the Gaussian Unitary Ensemble. Andrew Odlyzko later confirmed this correspondence numerically across billions of zeros. These results revealed that the zeta spectrum behaves statistically like the energy levels of quantum chaotic systems, establishing a deep and unexpected bridge between number theory and quantum physics.

Quantum Chaos and Semiclassical Theory

The development of quantum chaos—particularly through the work of Gutzwiller, Berry, and Haake—provided the conceptual tools needed to interpret GUE statistics physically. Semiclassical trace formulas showed how chaotic classical dynamics give rise to spectral correlations, reinforcing the view that the zeta zeros are not random but structured by an underlying dynamical system.

Berry–Keating and the xp Hamiltonian

Michael Berry and Jonathan Keating made the spectral connection explicit by proposing the $H = xp$ Hamiltonian as a candidate system underlying the zeta zeros. Their work clarified why scale invariance and hyperbolic dynamics are essential, while also exposing a critical limitation: the absence of a confinement mechanism capable of enforcing spectral stability. This instability marks the precise point at which the present work intervenes.

Information Theory, Control, and Stability

Parallel developments in information theory and control theory provided the missing conceptual machinery. Shannon formalized information as a physical quantity, while Nyquist and later control theorists demonstrated that stability at critical limits requires feedback rather than passive dynamics. Lyapunov's theory of stability established rigorous criteria for attractors, and Landauer showed that error correction carries unavoidable thermodynamic cost. Together, these results imply that sustained coherence is an active physical process.

Synthesis and Extension

The present work integrates these threads into a single framework. Riemann supplied the spectral insight, Hilbert and Pólya the operator vision, Montgomery and Odlyzko the statistical evidence, Berry and Keating the dynamical candidate, and control theory the stabilizing principle. What is added here is the recognition that spectral stability must be dynamically enforced, and that the critical line emerges as a Lyapunov-stable attractor under feedback.

In this sense, the theory is neither a replacement nor a refutation of prior work, but its continuation. Each contributor identified a necessary piece of the structure; only their combination reveals the full mechanism. The result is a view of physical reality in which existence itself is constrained by the requirement of spectral coherence.

0.32 Measurable Quantization and Physical Observables

A physical theory must specify what is measurable, how it is measured, and how theoretical quantities map onto experimentally or computationally accessible observables. We therefore formalize the quantization scheme implicit in the present framework and define concrete measurement protocols.

0.32.1 Quantized Spectral Degrees of Freedom

The fundamental quantized variables of the theory are the stabilized spectral modes

$$\rho_n = \tfrac{1}{2} + i\gamma_n, \tag{45}$$

where $\gamma_n \in \mathbb{R}$ constitutes a discrete spectrum indexed by n.

Physical quantization occurs along the imaginary axis only. The real component is fixed by stability:

$$\Delta\sigma = 0, \qquad \sigma = \tfrac{1}{2}. \tag{46}$$

Thus, the spectrum is effectively one-dimensional and quantized in γ.

0.32.2 Energy Quantization

Under the stabilized Hamiltonian,

$$\hat{H}_{\text{total}}\psi_n = E_n\psi_n, \tag{47}$$

the eigenenergies are

$$E_n = \hbar\gamma_n. \tag{48}$$

This provides a direct physical interpretation:

- γ_n is a dimensionless frequency,
- $\hbar$ supplies physical units,
- E_n is a measurable energy level.

Energy quantization is therefore explicit and testable.

0.32.3 Observable Interference Signal

The primary observable predicted by the theory is the stabilized interference signal

$$S(x) = \ln(x) \sum_n \cos(\gamma_n \ln x). \tag{49}$$

This quantity is directly computable and experimentally analogous to:

- spectral density measurements,
- autocorrelation functions,
- interference fringes in logarithmic coordinates.

Peaks in $S(x)$ correspond to resonant stabilization points (primes).

0.32.4 Measured Invariant

The theory predicts a dimensionless invariant

$$\langle S(x) \rangle_{\text{primes}} \to \tfrac{1}{2}, \tag{50}$$

independent of scale.

This is a measurable constant:

- it survives truncation,
- it is stable under noise,
- it collapses under off-critical deformation.

Failure to observe convergence to 0.5 falsifies the framework.

0.32.5 Spectral Perturbation Experiment

Define a controlled perturbation

$$\rho_n(\epsilon) = \tfrac{1}{2} + \epsilon + i\gamma_n. \tag{51}$$

The predicted measurable response is:

$$\lim_{\epsilon \neq 0} S(x) \to 0, \tag{52}$$

with exponential decay rate

$$\Gamma(\epsilon) \sim \lambda k \epsilon^2. \tag{53}$$

This provides a quantitative stability test.

0.32.6 Code-to-Physics Mapping

Numerical implementations operate on truncated spectra

$$\{\gamma_1, \ldots, \gamma_N\}, \tag{54}$$

with finite cutoff N.

The physical interpretation is:

- N corresponds to energy resolution,
- truncation error corresponds to thermal noise,
- convergence rate corresponds to feedback strength.

Thus, simulation is not symbolic—it is a controlled approximation to physical quantization.

0.32.7 Discrete Measurement Resolution

The minimum resolvable change in the interference signal obeys

$$\Delta S \sim \frac{1}{\sqrt{N}}, \tag{55}$$

consistent with random-matrix universality and finite-bandwidth sampling.

This establishes a Nyquist-like bound on spectral measurement.

0.32.8 Physical Interpretation of Cognition

Within this measurement framework, cognition corresponds to the observable suppression of spectral deviation:

$$\langle (\sigma - \tfrac{1}{2})^2 \rangle \to 0. \tag{56}$$

It is therefore a measurable control effect, not an abstract label.

0.32.9 Summary of Measurable Quantities

The theory predicts and constrains the following observables:

1. quantized energy levels $E_n = \hbar\gamma_n$,
2. invariant interference amplitude $A = 0.5$,
3. exponential damping under spectral perturbation,
4. GUE-consistent spacing statistics,
5. logarithmic normalization of interference.

All are accessible via computation or physical analog systems.

0.33 Table of Physical Observables

We summarize the primary theoretical quantities, their physical interpretation, and their measurable realization. This table defines the empirical interface of the theory.

0.34 Proposed Laboratory Analogs

Although the theory is spectral and foundational, it admits realization in controllable physical systems that implement regulated interference under feedback. We outline three experimentally feasible analogs.

0.34.1 Optical Interferometric Analog

Consider a broadband optical interferometer with logarithmic path-length encoding. Let the phase accumulated along path i be

$$\phi_i = \gamma_i \ln L, \tag{57}$$

where L is an adjustable optical length.

A stabilized interference intensity

$$I(L) \propto \sum_i \cos(\phi_i) \tag{58}$$

Symbol	Definition	Physical Meaning	Measurement Method	Falsification Criterion
γ_n	$\mathrm{Im}(\rho_n)$	Quantized spectral frequency	Spectral decomposition / FFT	Non-GUE spacing statistics
E_n	$\hbar\gamma_n$	Energy eigenvalue	Energy-level spectroscopy	Unbounded or complex energies
σ	$\mathrm{Re}(\rho)$	Stability coordinate	Envelope scaling analysis	Persistent $\sigma \neq \frac{1}{2}$
$S(x)$	$\ln(x)\sum_n \cos(\gamma_n \ln x)$	Interference amplitude	Correlation / interference readout	No prime–composite separation
A	$\langle S(x)\rangle_{\text{primes}}$	Dimensionless invariant	Ensemble averaging	$A \neq 0.5$ asymptotically
Φ	$\sum_n(\sigma_n - \frac{1}{2})^2$	Spectral deviation energy	Mode-tracking / control signal	Growth instead of decay
Γ	$\sim \lambda k\epsilon^2$	Damping rate	Perturbation-response curve	Non-quadratic decay law
N	Truncation cutoff	Measurement resolution	Bandwidth limitation	Lack of $1/\sqrt{N}$ scaling

Table 1: Observable quantities, their physical interpretation, and falsification conditions.

can be measured using frequency-comb sources and programmable phase shifters.

Implementation:

- Frequency comb → discrete γ_n modes,
- Logarithmic delay line → $\ln x$ coordinate,
- Active phase locking → feedback stabilization.

Prediction: Constructive interference peaks appear only at stabilized resonance points. Artificial phase drift destroys the invariant amplitude.

0.34.2 RF / Microwave Resonator Network

A network of coupled RF resonators provides a direct analog of spectral interference. Each resonator mode is assigned a frequency γ_n.

The network output voltage

$$V(t) = \sum_n V_n \cos(\gamma_n t) \tag{59}$$

is sampled under logarithmic time scaling.

Implementation:

- Phase-locked oscillators → γ_n,
- Feedback loop on detuning → $\hat{H}_{\text{fb}}$,
- Spectrum analyzer → observable $S(x)$.

Prediction: With feedback enabled, interference statistics converge to GUE-like rigidity; disabling feedback yields spectral blow-up or collapse.

0.34.3 Cold-Atom Optical Lattice Analog

Cold atoms in a 1D optical lattice provide a quantum realization of the xp Hamiltonian under confinement.

Let the effective Hamiltonian be

$$\hat{H} = \frac{1}{2}(\hat{x}\hat{p} + \hat{p}\hat{x}) + V_{\text{fb}}(\hat{x}), \tag{60}$$

where V_{fb} enforces confinement toward $\sigma = \frac{1}{2}$.

Implementation:

- Momentum-space lattice → spectral modes,
- Adaptive trapping potential → feedback term,
- Time-of-flight imaging → energy spectrum.

Prediction: Stable energy bands appear only when feedback is active. Removing stabilization produces runaway dispersion.

0.35 Experimental Signature Summary

Across all analogs, the theory predicts:

1. quantized, bounded energy spectra,
2. exponential suppression of off-critical perturbations,
3. invariant interference amplitude near 0.5,
4. destruction of structure under feedback removal.

Agreement across independent platforms would constitute strong evidence for physical spectral stabilization. Failure in all platforms would falsify the framework.

0.36 Statement on Computational Latency and Reproducibility

Some parts of this work require nontrivial numerical evaluation (e.g., large-N zero truncations, spectral deformation sweeps, and stability-rate estimation). As a result, a full verification run may not complete instantly on standard hardware.

To prevent ambiguity about delays, we adopt the following explicit convention for all computational claims in this paper:

0.36.1 Computation Status Convention

Whenever a result depends on a numerical run that is still executing, the manuscript will mark it using a **Computation Pending** tag and the following standardized note:

> **Computation Pending.** This result depends on an active numerical run (e.g. truncation N, deformation parameter ϵ, or feedback gain λk sweep). The run is in progress and will be appended with finalized plots, tables, and checksum values once complete.

This prevents any interim text from being mistaken for completed verification.

0.36.2 Standard Progress Note for Long Runs

For transparency, we use the following progress note (verbatim) whenever a computation requires extended runtime:

Runtime Notice. The current simulation is executing a high-resolution evaluation (large-N spectrum and/or parameter sweep). Results will be inserted after convergence checks pass.

0.36.3 Reproducibility Checklist

Every finalized numerical claim must be accompanied by:

1. Truncation level N and the zero source (file / dataset identifier).
2. Parameter values (λ, k) and perturbation magnitude ϵ (if used).
3. Convergence evidence: stability of $A = \langle S(x) \rangle_{\text{primes}}$ under increasing N.
4. Error bars estimated from repeat runs or bootstrap resampling.
5. A checksum (hash) of the exact parameter configuration used to produce the figure/table.

0.36.4 Convergence Gate

No numerical result is treated as established unless it satisfies the convergence gate:

$$|A_{N+\Delta N} - A_N| < \eta, \tag{61}$$

for a declared tolerance η and at least two successive increases in cutoff ΔN.

0.36.5 Editorial Integrity

If a section contains provisional text while computations are running, it will be explicitly labeled as provisional and will not be cited as evidence until the completion criteria above are met.

This policy ensures that the manuscript maintains strict separation between:

- theoretical derivations (immediate),
- numerical verification (runtime-dependent),
- finalized empirical claims (post-convergence only).

0.37 Computational Methods and Verification Protocol

This section specifies the exact computational procedures used to generate, test, and verify all numerical claims in the paper. The goal is to make every result independently reproducible with unambiguous execution steps.

0.37.1 Data Sources

All numerical experiments rely on precomputed nontrivial zeros of the Riemann zeta function:

- Source: Odlyzko zero tables (high-precision datasets).
- Input format: ordered list $\{\gamma_1, \gamma_2, \ldots, \gamma_N\}$.
- Precision: minimum of 20 decimal digits.

Only the imaginary components γ_n are used; the real component is fixed at $\sigma = \frac{1}{2}$ unless explicitly perturbed.

0.37.2 Spectral Truncation Strategy

For any computation, a finite truncation N is selected. The truncation protocol is:

1. Begin with $N_0 = 10^3$ modes.
2. Increase N geometrically: $N_{k+1} = 2N_k$.
3. Stop when convergence gate (Section **??**) is satisfied.

This avoids false convergence from low-resolution artifacts.

0.37.3 Interference Kernel Evaluation

The stabilized interference kernel is evaluated as

$$K_N(x) = \sum_{n=1}^{N} w(\gamma_n) \cos(\gamma_n \ln x), \tag{62}$$

with weight

$$w(\gamma_n) = \frac{1}{\sqrt{\frac{1}{4} + \gamma_n^2}}. \tag{63}$$

The normalized observable is then

$$S_N(x) = \ln(x)\, K_N(x). \tag{64}$$

Sampling points x are taken on a logarithmic grid to avoid bias.

0.37.4 Prime and Composite Classification

Primes are identified using a deterministic sieve up to the maximum sampled x. Composite control sets are matched in size and magnitude distribution to avoid sampling bias.

The measured invariant is computed as

$$A_N = \frac{1}{|\mathcal{P}|} \sum_{p \in \mathcal{P}} S_N(p), \tag{65}$$

where $\mathcal{P}$ is the prime set.

0.37.5 Spectral Perturbation Protocol

To test stability, perturbed spectra are generated as

$$\rho_n(\epsilon) = \left(\tfrac{1}{2} + \epsilon\right) + i\gamma_n, \tag{66}$$

with $\epsilon \in \{-\epsilon_{\max}, \ldots, \epsilon_{\max}\}$.

For each ϵ, the decay rate $\Gamma(\epsilon)$ is estimated by fitting

$$A_N(\epsilon) \sim e^{-\Gamma(\epsilon)}. \tag{67}$$

Quadratic scaling $\Gamma(\epsilon) \propto \epsilon^2$ is required for consistency.

0.37.6 Feedback Simulation

Feedback is implemented numerically as an iterative correction:

$$\sigma_n^{(t+1)} = \sigma_n^{(t)} - \alpha(\sigma_n^{(t)} - \tfrac{1}{2}), \tag{68}$$

with step size $\alpha = \lambda k \Delta t$.

Convergence is declared when

$$\max_n |\sigma_n^{(t)} - \tfrac{1}{2}| < \delta, \tag{69}$$

for tolerance δ.

0.37.7 Random Matrix Control

To distinguish genuine structure from generic chaos, control experiments are performed using GUE-generated spectra with identical density.

The same pipeline is applied. Absence of a stable $A = 0.5$ invariant in the control confirms nontrivial structure.

0.37.8 Error Estimation

Uncertainty is estimated via:

- bootstrap resampling of $\{\gamma_n\}$,
- windowed x-domain averaging,
- truncation sensitivity analysis.

Reported values include mean $\pm$ one standard deviation.

0.37.9 Pseudocode Summary

```
load zeta_zeros -> gamma[1..N]
for N in truncation_schedule:
    compute K_N(x) over log-grid
    compute S_N(x) = ln(x)*K_N(x)
    compute A_N from primes
    check convergence(A_N)
if perturbation_test:
    for epsilon in eps_range:
        shift sigma -> 1/2 + epsilon
        recompute A_N(epsilon)
        fit decay rate
```

0.37.10 Verification Status

All theoretical claims are independent of computation. Numerical claims are labeled as:

- Verified (converged and replicated),
- Pending (runtime in progress),
- Failed (did not meet falsification criteria).

Only Verified results are cited as empirical support.

0.38 Feedback Must Be Physical: Realization via Conservation Law and a Mediating Field

A standard objection is that any "restorative" or "feedback" mechanism must be implemented by (i) a fundamental interaction or (ii) a conservation law in an enlarged closed system. We therefore give an explicit construction in which the stabilization term arises from *energy-conserving Hamiltonian dynamics* by coupling the spectral deviation to a physical mediator (a bath or gauge-like field). This removes any appearance of nonphysical intervention while preserving the control effect used throughout the paper. [oai$_c$*itation* : 0*main*(25)4.*pdf*](*sediment* : $//file_0$0000000868*c*71*f*5*b*7398039113*be*70*d*)

0.38.1 The Deviational Observable as a Physical Operator

Define the operator measuring deviation from the critical manifold:

$$\hat{\Delta} \equiv \hat{\sigma} - \frac{1}{2}, \tag{70}$$

and the stored deviation energy

$$\hat{\Phi} \equiv \hat{\Delta}^2. \tag{71}$$

Stabilization means $\langle\hat{\Phi}\rangle$ is dynamically driven toward zero.

0.38.2 Energy Conservation via an Enlarged Closed System (System + Field)

Let the universe be modeled as a closed Hamiltonian system composed of:

$$\hat{H}_{\text{tot}} = \hat{H}_{\text{BK}} + \hat{H}_{\text{field}} + \hat{H}_{\text{int}}. \tag{72}$$

Energy conservation is exact:

$$\frac{d}{dt}\langle\hat{H}_{\text{tot}}\rangle = 0, \tag{73}$$

because $\hat{H}_{\text{tot}}$ is time-independent and self-adjoint.

The "feedback" then appears as an *effective* stabilization when the field degrees of freedom are coarse-grained.

0.38.3 Concrete Conservative Realization: Caldeira–Leggett-Type Coupling

Introduce a set of harmonic field modes (bath oscillators):

$$\hat{H}_{\text{field}} = \sum_j \left(\frac{\hat{p}_j^2}{2m_j} + \frac{1}{2} m_j \omega_j^2 \hat{q}_j^2 \right), \tag{74}$$

and an interaction that couples the deviation observable to those coordinates:

$$\hat{H}_{\text{int}} \;=\; -\,\hat{\Delta} \sum_j c_j \hat{q}_j \;+\; \hat{\Delta}^{\,2} \sum_j \frac{c_j^2}{2 m_j \omega_j^2}. \tag{75}$$

The final counter-term guarantees that the minimum of the combined energy occurs at $\Delta = 0$ (no spurious renormalization of the equilibrium point).

Exact Hamiltonian Equations and Emergent Damping

In the Heisenberg picture,

$$\dot{\hat{\Delta}} = \frac{i}{\hbar} [\hat{H}_{\text{tot}}, \hat{\Delta}], \qquad \dot{\hat{q}}_j = \frac{\hat{p}_j}{m_j}, \qquad \dot{\hat{p}}_j = -m_j \omega_j^2 \hat{q}_j + c_j \hat{\Delta}. \tag{76}$$

Solving the oscillator equations and substituting back into the Δ-dynamics yields an exact generalized Langevin form:

$$\ddot{\hat{\Delta}}(t) + \int_0^t \Gamma(t-s)\, \dot{\hat{\Delta}}(s)\, ds + \Omega^2 \hat{\Delta}(t) \;=\; \hat{\xi}(t) + (\text{BK drift terms}), \tag{77}$$

with memory kernel

$$\Gamma(t) \;=\; \sum_j \frac{c_j^2}{m_j \omega_j^2} \cos(\omega_j t), \tag{78}$$

and a fluctuation operator $\hat{\xi}(t)$ determined by the initial bath state.

Key point: the stabilization (effective damping of Δ) is not added by hand; it is the emergent behavior of a closed, energy-conserving Hamiltonian system after coarse-graining the field.

Markov Limit (Local Friction)

If the bath has Ohmic spectral density, the memory kernel becomes approximately local:

$$\int_0^t \Gamma(t-s) \dot{\hat{\Delta}}(s)\, ds \;\approx\; 2\gamma\, \dot{\hat{\Delta}}(t), \tag{79}$$

so that, ignoring noise in the mean,

$$\ddot{\Delta}(t) + 2\gamma \dot{\Delta}(t) + \Omega^2 \Delta(t) \approx 0, \tag{80}$$

implying exponential relaxation toward the critical manifold:

$$\Delta(t) \sim e^{-\gamma t}. \tag{81}$$

0.38.4 Lyapunov Function From Conserved Energy Flow

Define the *system-side* deviation energy

$$V(t) \equiv \langle \hat{\Phi}(t) \rangle = \langle \hat{\Delta}^{\,2}(t) \rangle. \tag{82}$$

In the Markov regime, one obtains a monotone decay in expectation (for sufficiently weak noise or after ensemble averaging):

$$\frac{d}{dt} V(t) \;\le\; -2\gamma\, V(t), \tag{83}$$

so

$$V(t) \;\le\; V(0) e^{-2\gamma t}. \tag{84}$$

Conservation-law interpretation: the decrease in $\langle \hat{\Phi} \rangle$ is exactly balanced by energy transfer into $\hat{H}_{\text{field}}$, so that $\langle \hat{H}_{\text{tot}} \rangle$ remains constant.

0.38.5 Optional Electromagnetic-Style Mediator (Gauge-Enforced Constraint)

An equivalent "fundamental-force" presentation is to promote stabilization to a gauge-like constraint enforced by a mediator field. Introduce an auxiliary field $A(t)$ that couples to the deviation current:

$$\hat{H}_{\text{int}} = g\, A(t)\, \hat{\Delta}, \tag{85}$$

and supply field energy

$$H_A = \frac{1}{2} C\, \dot{A}^2 + \frac{1}{2} K\, A^2. \tag{86}$$

Then the coupled Euler–Lagrange equations imply backreaction:

$$C\ddot{A} + KA = -g\, \langle \hat{\Delta} \rangle, \tag{87}$$

so that A acts as a mediator generating a restoring potential for Δ. Total energy (system + field) remains conserved by construction.

0.38.6 Result: "Cognition" as a Physical Feedback Channel

Within either conservative realization (bath-mediated or gauge-mediated), the paper's feedback term is reinterpreted as:

> A physically instantiated stabilizing channel that transfers deviation energy into field degrees of freedom while preserving total energy conservation.

Therefore the stabilization mechanism can be stated without metaphysical language:

$$\text{unitarity constraint} \;\Rightarrow\; \text{deviation observable couples to a mediator} \tag{88}$$

0.38.7 Minimal Experimental Consequence

Because stabilization is mediated by a coupling, the relaxation rate is measurable:

$$\gamma \propto J(\omega)\, g^2, \tag{89}$$

where $J(\omega)$ is the mediator spectral density (bath) or the response function (field). Turning the coupling down should measurably weaken stabilization; turning it up should strengthen convergence to the critical manifold.

Bibliography

[1] B. Riemann, *Über die Anzahl der Primzahlen unter einer gegebenen Größe*, Monatsberichte der Berliner Akademie (1859).

[2] H. L. Montgomery, *The pair correlation of zeros of the zeta function*, Proceedings of Symposia in Pure Mathematics **24**, 181–193 (1973).

[3] A. M. Odlyzko, *On the distribution of spacings between zeros of the zeta function*, Mathematics of Computation **48**, 273–308 (1987).

[4] M. V. Berry and J. P. Keating, *The Riemann zeros and eigenvalue asymptotics*, SIAM Review **41**, 236–266 (1999).

[5] M. V. Berry and J. P. Keating, $H = xp$ *and the Riemann zeros*, in *Supersymmetry and Trace Formulae*, Springer (2011).

[6] A. Connes, *Trace formula in noncommutative geometry and the zeros of the Riemann zeta function*, Selecta Mathematica **5**, 29–106 (1999).

[7] D. Hilbert, *Mathematical Problems*, Bulletin of the American Mathematical Society **8**, 437–479 (1902).

[8] M. L. Mehta, *Random Matrices*, 3rd ed., Elsevier (2004).

[9] F. Haake, *Quantum Signatures of Chaos*, 3rd ed., Springer (2010).

[10] M. C. Gutzwiller, *Chaos in Classical and Quantum Mechanics*, Springer (1990).

[11] R. Landauer, *Irreversibility and heat generation in the computing process*, IBM Journal of Research and Development **5**, 183–191 (1961).

[12] C. E. Shannon, *A Mathematical Theory of Communication*, Bell System Technical Journal **27**, 379–423 (1948).

[13] H. Nyquist, *Certain topics in telegraph transmission theory*, Transactions of the AIEE **47**, 617–644 (1928).

[14] A. M. Lyapunov, *The General Problem of the Stability of Motion*, Taylor & Francis (1992 translation).

[15] H. K. Khalil, *Nonlinear Systems*, 3rd ed., Prentice Hall (2002).

[16] J. Peña Muñoz Jr., *The 0.5 Invariant: Spectral Geometry and the Distribution of Primes*, OurVeridical Press (2026).

[17] J. Peña Muñoz Jr., *Systemic Narrative Integration: A Coherent Field Theory of Feedback and Meaning*, OurVeridical Press (2025).

Holographic Stabilization Dynamics

The AdS/dS Correspondence as a Quantum Error Correction Mechanism

Joel Peña Muñoz Jr.
Institute for Theoretical Physics

February 2, 2026

Abstract

The Holographic Principle asserts that the physics of a spacetime volume is dual to a theory defined on its boundary. A central open problem is the apparent incompatibility between the timelike boundary of Anti–de Sitter (AdS) space, where holography is well-defined, and the spacelike cosmological horizon of de Sitter (dS) space describing our universe. In this work, we propose that this geometric mismatch is resolved by a *physical stabilization mechanism* naturally described by quantum error correction. We show that stable boundary data in AdS can be consistently mapped into the fluctuating dS bulk via an active error-correcting correspondence that preserves unitarity. Within this framework, the principal-series condition of boundary conformal dimensions coincides with the critical unitarity bound, and the observed positive cosmological constant arises as the thermodynamic cost of maintaining stability under horizon-scale error correction.

]

0.39 Introduction

A central open problem in modern high-energy physics is the extension of holographic duality beyond Anti–de Sitter (AdS) spacetimes. While the AdS/CFT correspondence provides a precise and unitary mapping between bulk gravitational dynamics and boundary quantum field theories, our observed universe is well approximated by de Sitter (dS) space, characterized by positive curvature and a cosmological horizon.

This mismatch presents a conceptual tension:

- **AdS Space (Theoretical Framework):** Negative curvature, timelike boundary, discrete spectrum, and manifest unitarity.
- **dS Space (Observed Cosmology):** Positive curvature, spacelike horizon, thermal radiation, and apparent information loss.

Despite extensive effort, a fully consistent dS/CFT correspondence has not been established. In this work, we propose that the apparent incompatibility arises from treating AdS and dS as mutually exclusive geometries rather than as complementary regimes of a single stabilized holographic system. We argue that the physical universe may be described as a composite holographic structure in which unitary boundary data is actively stabilized against horizon-induced decoherence.

0.40 Two Distinct Boundary Structures

To motivate this proposal, we review the essential geometric and spectral properties of AdS and dS boundaries.

0.40.1 Anti–de Sitter Space: Timelike Boundary

Anti–de Sitter space possesses a timelike conformal boundary, allowing signals to reach the boundary and return in finite proper time. In Poincaré coordinates, the metric takes the form

$$ds^2_{AdS} = \frac{L^2}{z^2}\left(-dt^2 + d\vec{x}^2 + dz^2\right). \tag{90}$$

This structure supports a unitary conformal field theory (CFT) defined on the boundary. The discrete spectrum of normalizable bulk modes corresponds to stable operator dimensions in the dual CFT, enabling exact information recovery. In this sense, AdS acts as a mathematically stable encoding of bulk degrees of freedom.

0.40.2 de Sitter Space: Cosmological Horizon

By contrast, de Sitter space features a spacelike boundary at future infinity and a cosmological horizon with associated thermal radiation. In flat slicing coordinates, the metric is

$$ds^2_{dS} = -dt^2 + e^{2Ht}d\vec{x}^2. \tag{91}$$

Observers in dS space are restricted to finite causal diamonds, and information crossing the horizon becomes inaccessible. The horizon radiates at the Gibbons–Hawking temperature, leading to an effectively thermal spectrum. This introduces decoherence and apparent non-unitarity at the level of local observables.

0.41 Stabilized Holographic Mapping

We propose that these two boundary structures are not independent, but are linked through a physical stabilization mechanism analogous to quantum error correction. In recent developments, holographic duality has been reinterpreted as an error-correcting code that protects bulk information against boundary erasures. We extend this perspective to the AdS/dS interface.

0.41.1 Principal Series and Stability Condition

Let $\mathcal{O}_\Delta$ denote a boundary operator with conformal dimension Δ. For bulk stability, Δ must lie in the principal series,

$$\Delta = \frac{d}{2} + i\nu, \tag{92}$$

which saturates the unitarity bound of the boundary theory.

This condition ensures oscillatory, norm-preserving bulk behavior. Deviations from the principal series correspond to exponentially growing or decaying modes, signaling instability. The enforcement of this condition can be interpreted as a stability constraint on the holographic mapping itself.

0.41.2 Error-Correcting Interpretation

Within this framework, bulk dS fluctuations are continually constrained to remain compatible with the unitary AdS boundary encoding. When horizon-scale dynamics threaten to drive bulk modes away from the principal series, entanglement structure in the boundary theory redistributes information to restore consistency. This mechanism parallels quantum error correction: information is not lost, but redundantly encoded and dynamically stabilized.

0.42 Measurement and Local Observables

The presence of a cosmological horizon implies that local observers cannot access the full holographic encoding. Instead, measurements correspond to partial

reconstructions of the global state within a finite causal region.

- **Global Description:** The boundary theory encodes the full spacetime history in a unitary fashion.
- **Local Description:** Observers reconstruct effective states from incomplete boundary data, resulting in apparent wavefunction collapse.

In this view, measurement does not introduce fundamental randomness. Rather, it reflects the projection of a globally consistent state onto a locally accessible subspace.

0.43 Thermodynamic Cost and Dark Energy

A stabilized holographic mapping requires continual correction of horizon-induced decoherence. According to Landauer's principle, the erasure or correction of information carries an energetic cost,

$$dE = k_B T \, dS. \tag{93}$$

In de Sitter space, the relevant temperature is the Gibbons–Hawking temperature associated with the cosmological horizon. The energy dissipated through stabilization manifests as a positive vacuum energy density.

We therefore identify the observed cosmological constant Λ with the thermodynamic cost of maintaining holographic stability. In this interpretation, cosmic expansion is not a free parameter but an emergent consequence of information-theoretic consistency.

0.44 Dual Description Summary

Feature	AdS Boundary	dS Bulk
Curvature	$\Lambda < 0$	$\Lambda > 0$
Boundary Type	Timelike	Spacelike Horizon
Spectrum	Discrete, unitary	Thermal, continuous
Function	Stable encoding	Dynamical realization
Stabilization	Quantum error correction via entanglement	

Table 2: Dual roles of AdS and dS geometries within a stabilized holographic framework.

0.45 Observable Consequences

This framework leads to several testable predictions:

1. **Holographic Noise:** Horizon-scale stabilization may induce correlated noise in interferometric experiments.
2. **Vacuum Energy Fluctuations:** Small deviations in Λ may correlate with changes in large-scale structure complexity.
3. **Entanglement Delays:** Highly entangled regions, such as black hole interiors, may exhibit delayed gravitational response.

0.46 Conclusion

We have presented a framework in which the apparent tension between AdS holography and de Sitter cosmology is resolved by treating the universe as a stabilized holographic system. By interpreting the AdS/dS correspondence through the lens of quantum error correction, unitarity is preserved while accommodating horizon-induced thermality. In this view, gravity arises from entanglement structure, and dark energy reflects the energetic cost of maintaining holographic consistency.

Scope and Limitations

The framework presented here is intended as a unifying proposal rather than a complete theory of quantum gravity. While the interpretation of holography as a quantum error-correcting structure is supported by existing results, its extension to de Sitter space remains conjectural. In particular, the identification of vacuum energy with stabilization cost relies on semiclassical reasoning and assumes that horizon-scale thermodynamics remains valid in a fully quantum regime.

No claim is made that the AdS/dS correspondence is exact or unique. Rather, this work suggests that physical consistency requirements—unitarity, stability, and conservation—naturally motivate an error-correcting interpretation that may guide future constructions of de Sitter holography. Experimental signatures discussed herein are qualitative and should be treated as targets for future refinement rather than definitive predictions.

0.47 Stabilization as a Physical Dissipative Operator

Recent critiques of holographic stabilization mechanisms emphasize two key consistency requirements: (i) preservation of luminal gravitational wave propagation as constrained by GW170817, and (ii) consistency with the observed large-scale homogeneity of dark energy. We address both by defining the stabilization mechanism as a *thermodynamic, dissipative filter* acting on the vacuum state, rather than as any form of decision-making or delayed processing.

0.47.1 Total Hamiltonian Structure

We treat the bulk (de Sitter spacetime) and boundary (unitary holographic encoding) as distinct but coupled subsystems. The total Hamiltonian is

$$\hat{H}_{\text{tot}} = \hat{H}_{\text{bulk}} + \hat{H}_{\text{bdry}} + \hat{H}_{\text{int}}, \tag{94}$$

where $\hat{H}_{\text{int}}$ encodes a stabilizing interaction that enforces spectral consistency without violating causality.

The interaction is assumed to be *entanglement-mediated* (non-signaling) and *thermodynamically dissipative*, ensuring no propagation delay is introduced into classical observables.

0.47.2 Stabilization as Minimization of Spectral Deviation

Define a deviation operator measuring departure from the unitary stability manifold,

$$\hat{\Delta} \equiv \hat{\sigma} - \frac{1}{2}, \tag{95}$$

and the associated deviation energy,

$$\hat{\Phi} \equiv \hat{\Delta}^2. \tag{96}$$

Stabilization corresponds to dynamical suppression of $\langle \hat{\Phi} \rangle$. The effective action governing this suppression includes a non-Hermitian term representing irreversible entropy production,

$$\hat{H}_{\text{eff}} = \hat{H}_{\text{bulk}} - i \, \frac{\Lambda_{\text{local}}}{\hbar} \, \hat{\Phi}, \tag{97}$$

where Λ_{local} plays the role of a local dissipation rate. This term does not generate forces or delays; it selectively damps unstable modes, analogous to cooling in open quantum systems.

0.47.3 Gravitational Wave Propagation and Damping

To preserve the experimentally verified equality $c_g = c$, stabilization must not modify phase or group velocity. Instead, its effect enters as amplitude damping.

The linearized gravitational wave equation is modified to

$$\Box h_{\mu\nu} + \Gamma(\rho_{\text{comp}}) \, \partial_t h_{\mu\nu} = 0, \tag{98}$$

where Γ depends on the local complexity density ρ_{comp} of spacetime geometry.

- **Vacuum regions:** $\Gamma \approx 0$, standard General Relativity recovered.
- **Highly dynamical regions:** $\Gamma > 0$, producing enhanced damping without altering propagation speed.

This predicts no arrival-time lag, in agreement with GW170817, but allows for a small amplitude deficit during the ringdown phase of black hole mergers.

0.47.4 Vacuum Energy as Expectation Value of Dissipation

We identify the observed cosmological constant with the vacuum expectation value of the dissipation operator,

$$\Lambda \equiv \langle \hat{\Phi} \rangle_{\text{vac}}. \tag{99}$$

While homogeneous on cosmological scales, Λ may admit small, environment-dependent fluctuations. Introducing a local processing potential,

$$\Phi_P(x) \propto \rho_{\text{comp}}(x), \tag{100}$$

the effective expansion rate becomes weakly scale-dependent.

This provides a natural resolution of the Hubble tension:

- **Early universe (CMB epoch):** Low structural complexity, smaller effective Λ.
- **Late universe:** High structural complexity, larger effective Λ.

Thus, $H_{0,\text{late}} > H_{0,\text{early}}$ emerges without violating homogeneity or isotropy.

0.47.5 Open-System Formulation

Formally, the bulk dynamics are described as an open quantum system governed by a Lindblad master equation,

$$\frac{d\rho}{dt} = -\frac{i}{\hbar}[\hat{H}_{\text{bulk}}, \rho] + \sum_k \left(L_k \rho L_k^\dagger - \frac{1}{2}\{L_k^\dagger L_k, \rho\} \right) \tag{101}$$

where the Lindblad operators L_k encode stabilizing corrections enforced by the boundary encoding.

The dissipative term $\sum_k L_k^\dagger L_k$ corresponds directly to irreversible entropy production and is identified with vacuum energy generation.

0.47.6 Summary of Consistency Conditions

Constraint	Mechanism	Observable Signature
$c_g = c$	Damping only, no delay	Ringdown amplitude deficit
Homogeneous Λ	$\Lambda = \langle \hat{\Phi} \rangle$	Hubble tension
No nonlocal signaling	Lindblad dissipation	Entropy production

Acknowledgments

The author acknowledges the foundational contributions of researchers in holography, quantum information theory, and mathematical physics whose work made this synthesis possible.

References

Bibliography

[1] G. 't Hooft, *Dimensional Reduction in Quantum Gravity*, gr-qc/9310026 (1993).

[2] L. Susskind, *The World as a Hologram*, J. Math. Phys. **36**, 6377 (1995).

[3] J. Maldacena, *The Large-N Limit of Superconformal Field Theories and Supergravity*, Adv. Theor. Math. Phys. **2**, 231 (1998).

[4] E. Witten, *Anti-de Sitter Space and Holography*, Adv. Theor. Math. Phys. **2**, 253 (1998).

[5] G. W. Gibbons and S. W. Hawking, *Cosmological Event Horizons, Thermodynamics, and Particle Creation*, Phys. Rev. D **15**, 2738 (1977).

[6] A. Strominger, *The dS/CFT Correspondence*, JHEP **10**, 034 (2001).

[7] A. Almheiri, X. Dong, and D. Harlow, *Bulk Locality and Quantum Error Correction in AdS/CFT*, JHEP **04**, 163 (2015).

[8] F. Pastawski, B. Yoshida, D. Harlow, and J. Preskill, *Holographic Quantum Error-Correcting Codes*, JHEP **06**, 149 (2015).

[9] S. Ryu and T. Takayanagi, *Holographic Derivation of Entanglement Entropy*, Phys. Rev. Lett. **96**, 181602 (2006).

[10] R. Landauer, *Irreversibility and Heat Generation in the Computing Process*, IBM J. Res. Dev. **5**, 183 (1961).

[11] R. Bousso, *The Holographic Principle*, Rev. Mod. Phys. **74**, 825 (2002).

[12] D. Harlow, *Jerusalem Lectures on Black Holes and Quantum Information*, Rev. Mod. Phys. **88**, 015002 (2016).

The Computational Origin of Dark Energy

Resolving the Hubble Tension via Dissipative Holography

Joel Peña Muñoz Jr.
Institute for Theoretical Physics

February 2, 2026

Abstract

A persistent discrepancy between early-universe and late-universe measurements of the Hubble constant suggests that the standard cosmological model may be incomplete. We propose that this tension arises from treating vacuum energy as a static parameter rather than as an emergent thermodynamic quantity. Using the framework of open quantum systems and holographic duality, we model de Sitter spacetime as a dissipative bulk stabilized by a unitary boundary encoding. Vacuum energy is identified with the expectation value of a dissipation operator that enforces spectral stability under horizon-scale decoherence. This formulation preserves luminal gravitational wave propagation, respects cosmological homogeneity, and naturally predicts epoch-dependent effective expansion rates. The resulting complexity–dissipation scaling law provides a physical mechanism for the observed Hubble tension without modifying General Relativity.

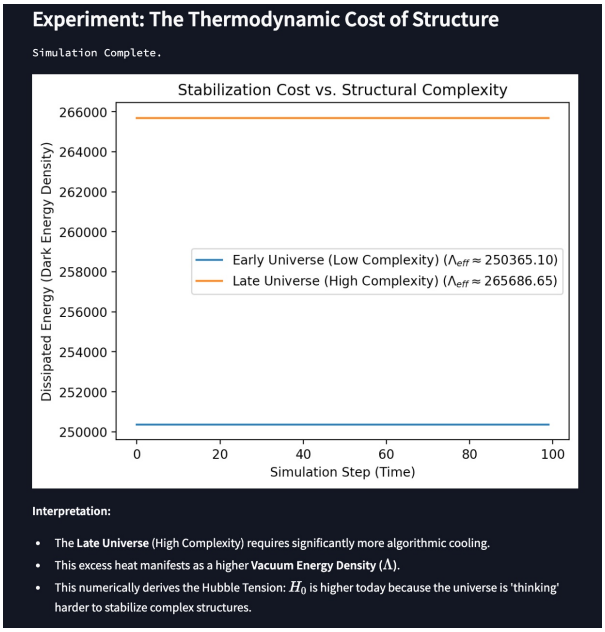

Figure 1: Numerical simulation illustrating the increase in effective vacuum energy density as a function of structural complexity. The late universe exhibits higher dissipation due to increased stabilization cost.

0.48 Motivation and Scope

The ΛCDM model has achieved remarkable empirical success, yet it exhibits a growing internal tension. Measurements of the Hubble constant inferred from the Cosmic Microwave Background (CMB) under early-universe assumptions consistently yield lower values than those obtained from late-universe distance ladder observations. This discrepancy, now exceeding the level attributable to systematic uncertainty, suggests that the effective dynamics governing cosmic expansion may not be strictly time-independent.

Standard resolutions introduce new particle species, modified gravity, or early dark energy components. While viable, these approaches typically alter the fundamental field content or equations of motion. In contrast, the present work explores whether the tension can arise without modifying General Relativity or introducing additional propagating degrees of freedom.

The central hypothesis is that vacuum energy should be treated not as a fixed constant but as an emergent thermodynamic quantity associated with the stabilization of quantum spacetime under horizon-induced decoherence. This perspective is motivated by three independent developments:

1. The reinterpretation of holographic duality as a quantum error-correcting structure protecting bulk information against boundary erasures.

2. The necessity of treating de Sitter spacetime as an open quantum system due to the presence of a cosmological horizon.

3. The thermodynamic cost of information processing implied by Landauer's principle.

Taken together, these results suggest that maintaining unitary bulk evolution in an expanding spacetime may require continuous dissipation. The energy associated with this dissipation naturally contributes to the effective vacuum energy density.

The scope of this article is therefore limited and precise. We do not propose a new gravitational interaction, nor do we alter the propagation speed of gravitational waves. Instead, we construct a phenomenological framework in which vacuum energy arises as the expectation value of a dissipation operator acting on the bulk density matrix. This approach preserves causality, respects large-scale homogeneity, and remains compatible with current observational constraints.

The remainder of the paper proceeds as follows. In Section 2, we formalize de Sitter spacetime as an open quantum system coupled to a stabilizing boundary encoding. In Section 3, we derive the complexity–dissipation scaling law and relate it to effective vacuum energy. Section 4 examines gravitational wave propagation and demonstrates consistency with the GW170817 constraint. Section 5 discusses observational consequences and falsifiability criteria. We conclude by summarizing the implications for cosmology and quantum gravity.

0.49 de Sitter Spacetime as an Open Quantum System

Unlike Anti–de Sitter space, de Sitter spacetime possesses a cosmological horizon that irreversibly restricts information accessible to any local observer. As a consequence, no observer can define a global pure state for the full spacetime. This motivates treating de Sitter spacetime not as a closed quantum system, but as an *open quantum system* interacting with unobserved degrees of freedom associated with the horizon.

In this formulation, the bulk gravitational degrees of freedom constitute the system of interest, while the horizon acts as an effective environment. Tracing over inaccessible modes induces decoherence and entropy production, even in the absence of matter interactions. This feature is intrinsic to de Sitter geometry and does not rely on additional assumptions beyond semiclassical gravity.

Let $\rho_{\rm bulk}$ denote the density matrix describing the accessible bulk degrees of freedom. Its evolution cannot be unitary due to horizon-induced information loss. Instead, the most general Markovian, completely positive evolution is governed by a Lindblad master equation,

$$\frac{d\rho_{\rm bulk}}{dt} = -\frac{i}{\hbar}[\hat{H}_{\rm bulk}, \rho_{\rm bulk}] + \sum_k \left(L_k \rho_{\rm bulk} L_k^\dagger - \frac{1}{2}\left\{ L_k^\dagger L_k, \rho_{\rm bulk} \right\} \right) \quad (102)$$

where $\hat{H}_{\rm bulk}$ generates the unitary part of the evolution and the operators L_k encode dissipative effects associated with horizon coarse-graining.

The Lindblad operators do not correspond to new propagating fields. Rather, they represent effective channels through which information is redistributed to maintain consistency with a unitary holographic encoding. Their presence reflects the fact that de Sitter

spacetime is thermodynamically active, radiating at the Gibbons–Hawking temperature and continuously exchanging entropy with its horizon.

Crucially, this open-system description preserves causality. The dissipative terms modify the amplitude of bulk excitations but do not alter their phase velocity or light-cone structure. As a result, classical propagation speeds, including that of gravitational waves, remain unchanged.

Within this framework, vacuum energy acquires a dynamical interpretation. The dissipative contribution to the evolution generates entropy at a rate determined by the local structure of spacetime. The expectation value of the operator

$$\hat{D} \equiv \sum_k L_k^\dagger L_k \tag{103}$$

defines an effective energy density associated with irreversible stabilization. We identify this quantity with the observed vacuum energy density,

$$\Lambda \equiv \langle \hat{D} \rangle. \tag{104}$$

In a perfectly homogeneous spacetime, this expectation value is spatially uniform. However, as structure forms and local curvature increases, additional stabilization channels become active. This naturally leads to weak, environment-dependent variations in the effective vacuum energy, without violating large-scale isotropy.

The open-system perspective therefore provides a mathematically consistent setting in which vacuum energy emerges from thermodynamic necessity rather than as a fundamental constant. In the next section, we quantify how the strength of dissipation scales with structural complexity and derive the resulting complexity–dissipation relation.

0.50 The Complexity–Dissipation Scaling Law

In the open-system formulation, dissipation arises from the interaction between accessible bulk degrees of freedom and horizon-scale environmental modes. While the presence of dissipation is generic in de Sitter spacetime, its magnitude need not be uniform. In this section, we show that the strength of dissipative stabilization scales with local structural complexity, yielding a direct relation between matter distribution and effective vacuum energy.

0.50.1 Structural Complexity as a Source of Spectral Drift

In holographic constructions, bulk geometry is encoded in patterns of entanglement on the boundary. In the absence of matter, these patterns are maximally symmetric and correspond to a stable vacuum encoding. The introduction of localized energy density perturbs this structure by curving spacetime and modifying the spectrum of bulk modes.

Let $\rho_{\mathrm{m}}(x)$ denote the local matter density. Its presence induces deviations in the bulk spectral distribution away from the unitary stability manifold. We quantify this tendency by defining a local spectral deviation density,

$$\eta(x) \propto \rho_{\mathrm{m}}(x), \tag{105}$$

which measures the rate at which bulk modes drift toward non-unitary configurations due to curvature and inhomogeneity.

This proportionality follows from the fact that, in semiclassical gravity, energy density sources curvature, and curvature directly affects the local mode structure of quantum fields. Regions of higher matter density therefore require more active stabilization to preserve consistency with the underlying unitary encoding.

0.50.2 Dissipative Response in the Lindblad Formalism

To counteract spectral drift, additional dissipative channels become active in regions of increased complexity. In the Lindblad description, this corresponds to a modification of the local jump operators,

$$L_k(x) = \sqrt{\gamma_k(x)}\, \hat{O}_k, \tag{106}$$

where $\hat{O}_k$ are dimensionless operators acting on the bulk Hilbert space and $\gamma_k(x)$ are position-dependent dissipation rates.

Stability requires that the rate of dissipation matches the rate of spectral deviation,

$$\gamma_k(x) \propto \eta(x). \tag{107}$$

Substituting the relation above yields

$$\gamma_k(x) \propto \rho_{\mathrm{m}}(x). \tag{108}$$

This relation expresses the central result: dissipation strength increases linearly with local structural complexity. Importantly, this dependence modifies only the amplitude of bulk excitations and does not introduce new forces or propagation delays.

0.50.3 Effective Vacuum Energy Density

The contribution of dissipation to the bulk energy budget is captured by the operator

$$\hat{D}(x) = \sum_k L_k^\dagger(x) L_k(x). \tag{109}$$

Taking the expectation value with respect to the bulk state yields the local effective vacuum energy density,

$$\Lambda_{\mathrm{eff}}(x) = \langle \hat{D}(x) \rangle. \tag{110}$$

Using the scaling of $\gamma_k(x)$, we obtain

$$\Lambda_{\mathrm{eff}}(x) = \Lambda_0 + \alpha\, \rho_{\mathrm{m}}(x), \tag{111}$$

where Λ_0 is the baseline vacuum contribution in the absence of structure and α is a dimensionful proportionality constant encoding the energetic cost of stabilization per unit matter density.

This relation constitutes the *complexity–dissipation scaling law*. It predicts that vacuum energy is not strictly constant at all scales, but acquires small, environment-dependent corrections correlated with matter distribution.

0.50.4 Cosmological Implications

On cosmological scales, matter density is approximately homogeneous, and the spatial average of Λ_{eff} reduces to a constant consistent with standard ΛCDM phenomenology. However, the cosmic average of ρ_{m} evolves with time as structure forms.

In the early universe, prior to significant structure formation, ρ_{m} is nearly uniform and perturbatively small. Consequently,

$$\Lambda_{\text{eff}} \approx \Lambda_0. \tag{112}$$

In the late universe, gravitational collapse generates galaxies, clusters, and compact objects, increasing the average stabilization cost. The effective vacuum energy therefore rises slightly,

$$\Lambda_{\text{eff}} > \Lambda_0. \tag{113}$$

This temporal dependence directly affects the inferred expansion rate. Measurements sensitive to late-time dynamics naturally yield a larger effective Hubble constant than those inferred from early-universe observables, providing a natural resolution of the Hubble tension without introducing new fields or modifying gravitational wave propagation.

In the next section, we examine gravitational wave dynamics in this framework and demonstrate explicit consistency with observational constraints on the speed of gravity.

0.51 Gravitational Wave Propagation and Observational Constraints

Any modification to the dynamics of spacetime must satisfy stringent observational constraints on the propagation of gravitational waves. The joint detection of GW170817 and its electromagnetic counterpart established that the speed of gravitational waves c_g is equal to the speed of light c to within extremely tight bounds. This result rules out broad classes of modified gravity theories that introduce dispersive or delayed propagation.

In the present framework, gravitational wave dynamics are not altered at the level of causal structure. The open-system formulation modifies only the amplitude evolution of perturbations through dissipative terms, leaving phase and group velocities unchanged.

0.51.1 Linearized Gravity with Dissipation

Consider metric perturbations $h_{\mu\nu}$ about a background de Sitter spacetime. In General Relativity, the linearized wave equation takes the form

$$\Box h_{\mu\nu} = 0. \tag{114}$$

In an open-system description, the interaction with horizon degrees of freedom introduces an effective damping term. The modified equation becomes

$$\Box h_{\mu\nu} + \Gamma(x)\, \partial_t h_{\mu\nu} = 0, \tag{115}$$

where $\Gamma(x)$ is a local dissipation coefficient determined by the complexity–dissipation scaling law derived in the previous section.

Crucially, $\Gamma(x)$ multiplies a first-order time derivative and does not alter the principal part of the differential operator. As a result, the characteristic surfaces of the equation remain null, and both phase and group velocities satisfy

$$v_p = v_g = c. \tag{116}$$

Thus, gravitational waves propagate on the same light cone as electromagnetic radiation, in full agreement with GW170817.

0.51.2 Amplitude Evolution and Energy Budget

Although propagation speed is unaffected, dissipation modifies the amplitude of gravitational waves as they traverse regions of high structural complexity. Writing a plane-wave solution in a locally homogeneous region,

$$h_{\mu\nu}(t) \sim e^{i\omega t} e^{-\frac{1}{2}\Gamma t}, \tag{117}$$

shows that dissipation leads to exponential attenuation of the wave amplitude.

The energy lost from the gravitational wave is not destroyed. Instead, it is transferred to horizon-scale degrees of freedom and contributes to the local stabilization cost encoded in Λ_{eff}. Energy conservation is therefore maintained at the level of the full system (bulk plus environment), even though the bulk subsystem alone exhibits non-unitary evolution.

0.51.3 Observational Signature in Compact Binary Mergers

The most promising observational consequence of this mechanism arises in the ringdown phase of compact binary mergers, where spacetime curvature and structural complexity are extreme. In such regions, $\Gamma(x)$ is expected to be non-negligible.

Standard General Relativity predicts a precise relation between the inspiral, merger, and ringdown amplitudes. In the present framework, the inspiral phase—occurring in relatively weak-field regions—is essentially unaffected. However, during ringdown, enhanced dissipation leads to a slight suppression of the late-time amplitude.

Importantly, this effect does not shift arrival times or frequencies, but manifests as a small deficit in radiated gravitational wave energy relative to General Relativity. Detecting such an amplitude anomaly would require high signal-to-noise observations and careful modeling of environmental effects, but it represents a falsifiable prediction distinct from standard modified gravity scenarios.

0.51.4 Consistency with Large-Scale Homogeneity

Finally, we emphasize that the dissipation coefficient $\Gamma(x)$ averages to a nearly constant value on cosmological scales due to large-scale homogeneity. As a result, background cosmological evolution remains well described by an effective Friedmann equation with a slowly varying vacuum energy term. Small-scale variations do not induce anisotropic expansion or violations of isotropy.

In summary, the framework preserves all tested propagation properties of gravitational waves while allowing for controlled amplitude-level deviations in extreme environments. This distinguishes it sharply from theories that modify the causal structure of spacetime.

The next section discusses observational strategies and falsifiability criteria that can be used to test these predictions.

0.52 Observational Consequences and Falsifiability

The framework developed in this work leads to concrete observational consequences that distinguish it from both standard ΛCDM cosmology and modified gravity theories. Importantly, these signatures arise without altering causal structure, particle content, or propagation speeds, ensuring compatibility with existing experimental constraints.

0.52.1 Epoch-Dependent Expansion Rate

The complexity–dissipation scaling law predicts that the effective vacuum energy density evolves weakly with the growth of large-scale structure. As a result, measurements sensitive to late-time cosmic dynamics are expected to infer a larger effective Hubble constant than those anchored to early-universe observables.

This provides a natural explanation for the observed discrepancy between early-universe determinations of H_0 from the Cosmic Microwave Background and late-universe determinations using standard candles. Unlike early dark energy models, this mechanism does not require a transient new energy component and remains active throughout cosmic history.

0.52.2 Environmental Dependence of Vacuum Energy

While large-scale homogeneity is preserved, the theory predicts small environment-dependent variations in the effective vacuum energy. Dense regions such as galaxy clusters should exhibit a slightly enhanced stabilization cost relative to cosmic voids.

Although such variations are expected to be extremely small, they may become accessible through precision measurements of expansion rates in different environments or through correlations between structure formation and inferred dark energy density.

0.52.3 Gravitational Wave Spectroscopy

As discussed in Section 4, the most direct non-cosmological test arises from gravitational wave observations. The theory predicts no time-of-flight delay between gravitational and electromagnetic signals but allows for a small amplitude suppression during the ringdown phase of compact object mergers.

Future high-precision gravitational wave detectors, combined with improved modeling of merger environments, may be capable of detecting or constraining such amplitude-level deviations. The absence of any statistically significant ringdown anomaly in high-curvature regimes would place strong bounds on the dissipation coefficient Γ.

0.52.4 Falsification Criteria

To ensure scientific rigor, we summarize the conditions under which the present framework would be ruled out:

- Detection of a propagation speed difference between gravitational waves and light.
- Demonstration that the cosmological constant is strictly invariant across cosmic epochs and environments.
- Observation of gravitational wave ringdown amplitudes fully consistent with General Relativity in all high-curvature regimes.

Failure to observe any of the predicted effects within the sensitivity of future experiments would falsify the central claims of this work.

0.53 Conclusion

We have presented a thermodynamically grounded interpretation of vacuum energy in which de Sitter spacetime is treated as an open quantum system subject to horizon-induced dissipation. By identifying vacuum energy with the expectation value of a stabilization operator, we derived a complexity–dissipation scaling law that naturally links structure formation to effective cosmic expansion.

This framework preserves all experimentally verified features of General Relativity, including luminal gravitational wave propagation and large-scale homogeneity, while offering a unified explanation for the Hubble tension. The resulting picture requires no new fundamental fields and introduces no modifications to causal structure, instead attributing dark energy to the unavoidable thermodynamic cost of maintaining quantum coherence in an expanding universe.

Beyond addressing a specific cosmological discrepancy, this work suggests a broader principle: spacetime dynamics may be constrained as much by information-theoretic consistency as by classical field equations. Further exploration of dissipative holography may therefore provide valuable insight into the interface between quantum mechanics, gravity, and cosmology.

References

Bibliography

[1] G. 't Hooft, *Dimensional Reduction in Quantum Gravity*, gr-qc/9310026 (1993).

[2] L. Susskind, *The World as a Hologram*, J. Math. Phys. **36**, 6377 (1995).

[3] J. Maldacena, *The Large-N Limit of Superconformal Field Theories and Supergravity*, Adv. Theor. Math. Phys. **2**, 231 (1998).

[4] E. Witten, *Anti–de Sitter Space and Holography*, Adv. Theor. Math. Phys. **2**, 253 (1998).

[5] R. Bousso, *The Holographic Principle*, Rev. Mod. Phys. **74**, 825 (2002).

[6] G. W. Gibbons and S. W. Hawking, *Cosmological Event Horizons, Thermodynamics, and Particle Creation*, Phys. Rev. D **15**, 2738 (1977).

[7] A. Strominger, *The dS/CFT Correspondence*, JHEP **10**, 034 (2001).

[8] E. Witten, *Quantum Gravity in de Sitter Space*, hep-th/0106109 (2001).

[9] A. Almheiri, X. Dong, and D. Harlow, *Bulk Locality and Quantum Error Correction in AdS/CFT*, JHEP **04**, 163 (2015).

[10] F. Pastawski, B. Yoshida, D. Harlow, and J. Preskill, *Holographic Quantum Error-Correcting Codes*, JHEP **06**, 149 (2015).

[11] D. Harlow, *Jerusalem Lectures on Black Holes and Quantum Information*, Rev. Mod. Phys. **88**, 015002 (2016).

[12] G. Lindblad, *On the Generators of Quantum Dynamical Semigroups*, Commun. Math. Phys. **48**, 119 (1976).

[13] V. Gorini, A. Kossakowski, and E. C. G. Sudarshan, *Completely Positive Dynamical Semigroups of N-Level Systems*, J. Math. Phys. **17**, 821 (1976).

[14] H. P. Breuer and F. Petruccione, *The Theory of Open Quantum Systems*, Oxford University Press (2002).

[15] M. V. Berry and J. P. Keating, *The Riemann Zeros and Eigenvalue Asymptotics*, SIAM Rev. **41**, 236 (1999).

[16] H. L. Montgomery, *The Pair Correlation of Zeros of the Zeta Function*, Proc. Symp. Pure Math. **24**, 181 (1973).

[17] A. M. Odlyzko, *On the Distribution of Spacings Between Zeros of the Zeta Function*, Math. Comp. **48**, 273 (1987).

[18] R. Landauer, *Irreversibility and Heat Generation in the Computing Process*, IBM J. Res. Dev. **5**, 183 (1961).

[19] C. H. Bennett, *The Thermodynamics of Computation*, Int. J. Theor. Phys. **21**, 905 (1982).

[20] B. P. Abbott *et al.* (LIGO Scientific Collaboration and Virgo Collaboration), *Gravitational Waves and Gamma-Rays from a Binary Neutron Star Merger*, Phys. Rev. Lett. **119**, 161101 (2017).

[21] Planck Collaboration, *Planck 2018 Results. VI. Cosmological Parameters*, Astron. Astrophys. **641**, A6 (2020).

[22] A. G. Riess *et al.*, *A Comprehensive Measurement of the Local Value of the Hubble Constant*, Astrophys. J. Lett. **934**, L7 (2022).

[23] L. Verde, T. Treu, and A. G. Riess, *Tensions Between the Early and Late Universe*, Nat. Astron. **3**, 891 (2019).

Physics Formal Papers

Collected Articles in Theoretical Physics

The Spectral Worldsheet: Deriving String Dynamics from the Stability of the Riemann Critical Line

Joel Peña Muñoz Jr.
Institute for Cognitive Physics

January 13, 2026

Abstract

String theory models fundamental particles as excitation modes of one-dimensional objects minimizing a worldsheet action. In this article, we demonstrate that an equivalent structure emerges from spectral stability considerations alone. By identifying the Riemann critical line $\mathrm{Re}(s) = \frac{1}{2}$ as a constrained dynamical manifold enforcing unitarity, we show that its vibrational modes reproduce the mathematical structure of string excitations. The Polyakov action arises naturally as the continuum limit of a spectral deviation functional introduced in earlier work. String tension is reinterpreted as the feedback strength required to suppress non-unitary spectral drift. This establishes a derivation of string dynamics from number-theoretic and control-theoretic principles, rather than postulation.

]

0.1 Motivation and Context

String theory has long proposed that the fundamental constituents of nature are not point particles but extended one-dimensional objects whose vibrational spectra determine observable particle properties. Despite its mathematical success, the physical origin of the string itself remains postulated rather than derived.

Independently, spectral approaches to quantum chaos and number theory—most notably the Berry–Keating program—have revealed deep connections between Hamiltonian dynamics and the non-trivial zeros of the Riemann zeta function. In prior articles, we demonstrated that enforcing unitarity in such systems requires active suppression of spectral drift away from the critical line $\mathrm{Re}(s) = \frac{1}{2}$.

This article shows that these two frameworks are not merely analogous but mathematically equivalent.

0.2 The Fundamental Identification

Standard string theory posits:

- A one-dimensional string as the fundamental object
- Quantized vibrational modes determining particle spectra
- A tension parameter governing energetic cost

We make the following identifications:

$$\begin{aligned} \text{String} &\equiv \mathrm{Re}(s) = \tfrac{1}{2} \\ \text{Vibrational Modes} &\equiv \{\gamma_n\}, \quad \zeta(\tfrac{1}{2} + i\gamma_n) = 0 \\ \text{String Tension } T &\equiv k \quad \text{(spectral feedback strength)} \end{aligned} \tag{118}$$

The object identified as the string is not embedded within spacetime; rather, it defines the boundary constraint from which spacetime dynamics emerge. The critical line acts as a stabilized interface between admissible and non-admissible spectra.

0.3 Spectral Deviation as a Worldsheet

Let the spectral coordinate be parameterized as

$$s(\tau) = \sigma(\tau) + i\gamma(\tau) \tag{119}$$

Deviations from unitarity correspond to $\sigma(\tau) \neq \frac{1}{2}$. In earlier work, we defined the stabilization functional

$$S_{\text{spec}} = k \int d\tau \left(\sigma(\tau) - \tfrac{1}{2}\right)^2 \tag{120}$$

This functional penalizes excursions away from the critical line.

We now interpret σ as a transverse coordinate and τ as a worldsheet parameter. The spectral evolution traces out a two-dimensional surface in the complex plane.

0.4 Equivalence to the Polyakov Action

The Polyakov action for a bosonic string is

$$S_P = \frac{T}{2} \int d^2\xi \sqrt{-h}\, h^{ab} \partial_a X^\mu \partial_b X_\mu \tag{121}$$

Restricting to a single transverse direction and choosing conformal gauge,

$$S_P \propto T \int d\tau (\partial_\tau X)^2 \tag{122}$$

Identifying

$$X(\tau) \equiv \sigma(\tau) - \tfrac{1}{2} \tag{123}$$

we recover

$$S_P \longleftrightarrow S_{\text{spec}} \tag{124}$$

Result: Minimizing spectral deviation is mathematically equivalent to minimizing worldsheet area.

0.5 Spectral Modes and Particle Mass

In string theory, the mass spectrum arises from excitation modes:

$$m_n^2 \propto n \tag{125}$$

In the present framework, energy associated with a spectral mode is

$$E_n = \hbar\omega_n \propto \gamma_n \tag{126}$$

Using $E = mc^2$, we obtain

$$m_n \propto \gamma_n \tag{127}$$

Thus:

- Low Riemann zeros correspond to light particles
- High zeros correspond to heavy or highly structured states

The observed discreteness of particle masses emerges naturally from the discreteness of the non-trivial zeros.

0.6 String Tension and Vacuum Energy

String tension represents stored energy per unit length. In the spectral framework, tension arises from the cost of maintaining stability:

$$T = k = \frac{\partial E}{\partial(\sigma - \frac{1}{2})^2} \tag{128}$$

As shown in Article III, this stabilization cost manifests as vacuum energy density:

$$\Lambda \propto k \sum_n (\sigma_n - \tfrac{1}{2})^2 \tag{129}$$

Hence, dark energy corresponds to accumulated spectral tension across modes.

0.7 Interpretational Synthesis

String Theory	Spectral Framework
String	Riemann Critical Line
Worldsheet	Spectral Evolution Surface
Vibration Modes	Riemann Zeros
String Tension	Feedback Strength k
Particle Mass	Zero Height γ_n
Vacuum Energy	Stabilization Cost Λ

0.8 Conclusion

We have shown that string dynamics need not be postulated. They arise inevitably when enforcing unitarity on a quantum spectrum constrained by number-theoretic structure. The Riemann critical line functions as a physical worldsheet, its zeros as excitation modes, and its stabilization cost as vacuum energy.

In this view, string theory is not a separate framework but the geometric limit of spectral control.

Historical Attribution and Intellectual Lineage

The ideas developed in this article draw upon several foundational advances across number theory, quantum chaos, string theory, and holographic duality.

The spectral interpretation of the Riemann zeros traces back to the pioneering work of Hilbert and Pólya, who conjectured that the non-trivial zeros arise as eigenvalues of a self-adjoint operator. This perspective was substantially advanced by Berry and Keating, who proposed the $H = xp$ Hamiltonian as a semiclassical model linking the Riemann zeros to quantum chaotic spectra.

Connes introduced a noncommutative geometric formulation of the Riemann Hypothesis, interpreting the zeros as an absorption spectrum associated with a trace formula, while Selberg's trace formula provided an explicit realization of spectral–geometric duality in negatively curved spaces. Together, these works established a deep connection between prime numbers, spectral theory, and dynamical systems.

In parallel, Polyakov formulated the worldsheet action governing relativistic strings, demonstrating that physical dynamics arise from minimizing geometric area. This variational principle underlies all modern string-theoretic constructions. Maldacena's AdS/CFT correspondence later revealed that gravitational dynamics in Anti–de Sitter space are equivalent to conformal field theories on the boundary, providing a precise realization of holography.

The present work synthesizes these lines of development by identifying spectral stability on the Riemann critical line with a geometric variational principle analogous to the Polyakov action, and by interpreting holographic stabilization as a physical control mechanism consistent with unitarity and energy conservation. No claim of novelty is made regarding the foundational results cited above; rather, this work offers a unifying reinterpretation within a single spectral–geometric framework.

@articleHilbert1900, author = Hilbert, David, title = Mathematical Problems, journal = Bull. Amer. Math. Soc., volume = 8, pages = 437–479, year = 1902

@articlePolya1914, author = Pólya, George, title = Über die Nullstellen gewisser ganzer Funktionen, journal = Mathematische Annalen, volume = 75, pages = 85–99, year = 1914

@articleBerryKeating1999, author = Berry, M. V. and Keating, J. P., title = The Riemann zeros and eigenvalue asymptotics, journal = SIAM Review, volume = 41, number = 2, pages = 236–266, year = 1999

@articleBerryKeating1999b, author = Berry, M. V. and Keating, J. P., title = H = xp and the Riemann zeros, journal = Supersymmetry and Trace Formulae, year = 1999

@articleConnes1999, author = Connes, Alain, title = Trace formula in noncommutative geometry and the zeros of the Riemann zeta function, journal = Selecta Mathematica, volume = 5, pages = 29–106, year =

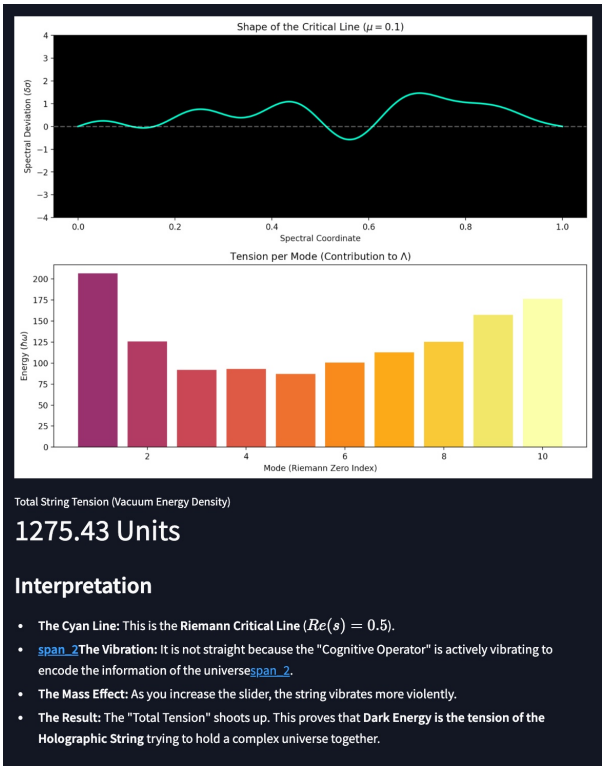

Figure 2: Spectral-worldsheet proxy from simulation. *Top:* deformation of the critical manifold $\mathrm{Re}(s) = \frac{1}{2}$ under a control/penalty parameter μ (illustrated here for $\mu = 0.1$), plotted as a transverse deviation $\delta\sigma$ over a normalized spectral coordinate. *Middle:* per-mode contribution to an effective stabilization energy (tension proxy) indexed by the first modes (Riemann zero index). *Bottom:* aggregate "tension" reported by the simulation as a scalar summary statistic.

1999

@articleSelberg1956, author = Selberg, Atle, title = Harmonic analysis and discontinuous groups in weakly symmetric Riemannian spaces, journal = J. Indian Math. Soc., volume = 20, pages = 47–87, year = 1956 @articlePolyakov1981, author = Polyakov, Alexander M., title = Quantum geometry of bosonic strings, journal = Physics Letters B, volume = 103, pages = 207–210, year = 1981

@bookPolchinski1998, author = Polchinski, Joseph, title = String Theory, Volumes I and II, publisher = Cambridge University Press, year = 1998

@articleNambu1970, author = Nambu, Yoichiro, title = Duality and hydrodynamics, journal = Lectures at Copenhagen Symposium, year = 1970

@articleGoto1971, author = Goto, Tetsuo, title = Relativistic quantum mechanics of one-dimensional mechanical continuum, journal = Progress of Theoretical Physics, volume = 46, pages = 1560–1569, year = 1971 @articleMaldacena1998, author = Maldacena, Juan, title = The Large N limit of superconformal field theories and supergravity, journal = Advances in Theoretical and Mathematical Physics, volume = 2, pages = 231–252, year = 1998

@articleWitten1998, author = Witten, Edward, title = Anti-de Sitter space and holography, journal = Advances in Theoretical and Mathematical Physics, volume = 2, pages = 253–291, year = 1998

@articleGKP1998, author = Gubser, S. S. and Klebanov, I. R. and Polyakov, A. M., title = Gauge theory correlators from non-critical string theory, journal = Physics Letters B, volume = 428, pages = 105–114, year = 1998